Assiut Veterinary Medical Journal Assiut Vet. Med. J. Vol. 71 No. 187 October 2025, 181-190

10.21608/avmj.2025.369484.1638 Assiut University web-site: www.aun.edu.eg

MAGNETIC RESONANCE IMAGING OF THE PINEAL GLAND IN DONKEY (*EQUUS ASINUS*)

MOHAMED KAMAL MERAI ABDEL MAKSOUD [1]; HEWA MOHAMMAD ALI [2]; AZZA ALI HASSAN IBRAHIM [1] AND HEBATALLAH HAMDY MAHMOUD [1]

[1] Anatomy and Embryology Department, Faculty of Veterinary Medicine, Beni-Suef University, Beni-Suef 62511, Egypt.
mkamalvet@gmail.com; mohamed.abdallah@vet.bsu.edu.eg.https://orcid.org/0000-0002-6723-9337
[2] Department of Biology, College of Education, Salahaddin University-Erbil, 44001, Iraq.

Received: 7 April 2025; **Accepted:** 1 July 2025

ABSTRACT

The mammalian pineal gland, a photo-neuroendocrine gland, regulates the circadian rhythm and reproductive activity in seasonally breeding animals. The current study aimed to clarify the morphometric features of the pineal gland and evaluate its normal MRI characteristics using variable MRI sequences in donkeys. We used twenty-two cadaveric heads from slaughtered adult donkeys with no abnormal neurological signs. Two heads were scanned using a 1.5 tesla MRI magnet in three sequences (T1-weighted, T2-weighted, Flair) and then preserved in a 10% formalin solution for ten days. The brains of these preserved heads were sectioned into sagittal and transverse slices. The brains of the other twenty heads were carefully extracted, and their weight, length, width, and height were measured. The pineal gland width, length, and height of these samples were also measured and correlated to the animal's sex and age, brain size, and body weight using different statistical tests. The mean pineal gland size was 1.23 ±0.13 cm length, 0.32 ±0.11 cm width, and 0.62 ±0.20 cm height. There was no significant difference detected between gland size and the animal's sex and age, brain size, or body weight (P>0.05). The gross sections of the brain aided in the morphological description of the pineal gland, including its color, shape, position, and relations. Moreover, using variable sequences of MRI enabled a comprehensive evaluation of the pineal gland with different intensities. These anatomical features of the pineal gland could be used as a standard anatomic reference for further interpretation of the pineal diseases in donkeys.

Key words: Donkey, Magnetic resonance imaging (MRI), Pineal gland.

INTRODUCTION

The pineal gland is found in the vertebrate brain, and its anatomy and location vary between species (Klein, 2015). In upper primates and ungulates, it is located in the epithalamus and communicates with the third ventricle through the pineal recess (Falcon, et al., 2009). The importance of this gland lies in the secretion of melatonin that is involved in rhythmic regulation of several phenomena related to the circadian cycle (Simonneaux and Ribelayga, 2003), besides, it plays an important role in regulating the reproductive

Corresponding author: Abdel Maksoud, M.K.M.
E-mail address: mohamed.abdallah@vet.bsu.edu.eg
Present address: Anatomy and Embryology Department, Faculty of Veterinary Medicine, Beni-Suef University, Beni-Suef 62511, Egypt.

activity in seasonally breeding animals (Bolat *et al.,* 2018). Furthermore, this gland is currently thought to act as a regulator gland that alters the activity of the gonads, parathyroid, adrenal glands, pancreatic islets, and neurohypophysis (Koshy and Vettivel, 2001). It was found that the disturbance of melatonin secretion caused by a diseased pineal gland resulted in disturbance of circadian rhythm, gonadal development, secondary sexual characteristics, and estrous cycle (Frandson *et al.,* 2009). Accordingly, it was of utmost concern to understand the normal morphology and imaging features of the pineal gland.

MRI is increasingly used for visualization and evaluation of various soft tissue structures (Werpy, 2004), due to its high resolution and superior contrast between soft structures without ionizing radiation (Peterfy *et al.,* 1994). As MRI becomes more widely available, it is more executable clinically to evaluate the equine brain (Schmidt *et al.,* 2019). Recent trends using MRI as a diagnostic tool for earlier detection of the pineal tumours are further growing in human clinics (Phuttharak *et al.,* 2023). Recognition of normal MRI features of the pineal gland is preliminary for a precise identification and assessment of the pineal diseases. Even though the histological features of the pineal gland are thoroughly described in several animal species: donkey (Ozgel *et al.,* 2008; Ebada, 2012), horse (Bolat *et al.,* 2018), cattle (Phillips *et al.,* 1989), buffalo (Carvalho *et al.,* 2009), sheep (Dahran and Ghonimi, 2023), goat (Hussain *et al.,* 2023), and dog (Calvo *et al.,* 1988), only few literature was available describing the normal MRI appearance of the pineal gland, especially in donkey. Consequently, the current study aimed to fully describe the normal MRI characteristics of the pineal gland in adult donkeys and to correlate the pineal gland size to sex, age, brain size, and body weight.

MATERIALS AND METHODS

Animals

The current study was a prospective cadaveric investigation that involved twenty-two heads of adult donkeys of both sexes. These heads were collected from Beni-Suef Zoo after the slaughtering of the donkeys for purposes unrelated to the study. Prior to slaughtering, the animals were grossly inspected and examined to ascertain that they were free from any neurological disorders; also, the sex, weight, and age of each animal were recorded. After slaughtering, the heads were dislocated at the level of the atlanto-axial joint, cleansed with tap water, and stored in an ice box at -4 ºC. This study was approved by the Institutional Animal Care and Use Committee of Beni-Suef University, Egypt (BSU-IACUC, Permit Number: 024-078).

Magnetic resonance imaging

Two heads were scanned 6 hours after slaughtering. These heads were located where their ventral aspects contacting the scanning table. Using a 1.5 Tesla magnet MRI scanner (Philips Intera; Philips GmbH, Hamburg, Germany), the heads were scanned in three sequences: T1-weighted, T2-weighted, and Flair spin-echo magnet in two successive planes, sagittal and transverse. The sagittal images were obtained parallel to the interparietal bone and perpendicular to the occipital bone, while the transverse images were obtained perpendicular to the temporomandibular joint. MRI settings for T1-weighted images were, an acquisition time (Acq Tm) of 21:14 minutes: seconds, a repetition time (RT) of 486 milliseconds, echo delay time (TE) of 140 milliseconds, field of view (FOV) of 21×21 mm, slice thickness of 5 mm, interstice space of 1mm, matrix size of 212×17, for T2-weighted images were, an acquisition time (Acq Tm) of 21:12 minutes: seconds, a repetition time (RT) of 540 milliseconds, echo delay time (TE) of 150 milliseconds, filed of view (FOV) of 24×24 mm, slice thickness of 5 mm, interstice space of 1mm, matrix size of 268 × 250, for Flair images were, an acquisition time (Acq Tm) of 21:15 minutes: seconds, a repetition time (RT) of 540 milliseconds, echo delay time (TE) of 150 milliseconds, field of view (FOV) of 25×25 mm, slice thickness of 5 mm, interstice space of 1mm, matrix size of 192 × 148. 60 transverse MR images (20 T1, 20 T2, 20 Flair), and 54 sagittal MR images (18 T1, 18 T2, 18 Flair) were obtained. These images were grossly inspected, and the intensity of each structure of the brain tissue was reported. Moreover, the position, relations, and tissue intensity of the pineal gland were recorded.

Preparation of the anatomic sections

The scanned heads (n=2) were used for anatomic sectioning of the brain. The common carotid artery of these specimens was injected with 10% formalin solution, and then they were preserved in 10% formalin solution for ten days. After extraction of the brains from the skull, they were sectioned in 2 cm thickness using a sharp knife into sagittal (n=1) and transverse (n=1) slices. The anatomic slices were successively numbered and grossly inspected and identified.

Gross morphology

Twenty fresh heads of cadaveric donkeys (10 males and 10 non-pregnant females) were used for gross inspection and morphometric analysis of the brain and pineal gland. For each head, the brain was gently extracted from the skull, and the cerebral cortex in each brain was gently dissected until reaching the pineal gland, which was grossly inspected and identified.

Statistics

The grossly investigated brain specimens (n=20) were measured and recorded in cm: length, width, and height. The parameters of their pineal glands were also measured, length, width, and height in cm. Mean and standard deviation were calculated for animals' age and weight, pineal gland measurements, and brain measurements. A one-way ANOVA test was used to calculate the significant difference between the pineal gland parameters (length, width, and height) and animal sex and age, brain parameters (length, width, and height), and body weight. All statistical analyses were achieved using statistics software (SPSS Statistics IBM, 2020; Aromonk, New York).

RESULTS

The obtained MR images were thoroughly reviewed for identification of the anatomic structures of the brain in several planes for each MRI sequence. Based on the anatomic description of the pineal gland, two MR images in each sequence were selected, matching the anatomic sections in two planes: one in a sagittal plane (Figure 1) and one in a transverse plane (Figure 2). Both planes were selected at the level of the interthalamic adhesion.

Statistical analysis

The results concerning the measurements of the brain and pineal gland in twenty donkeys (Table 1) revealed that the mean age was 12.7 ± 3.08 years and the mean weight was 176.60 ± 17.03 Kg. Also, the mean size of the brain was 13.89 ± 0.21 cm length, 8.99 ± 035 cm width, and 6.16 ± 0.21cm height. The mean size of the pineal gland was 1.23 ±0.13 cm length, 0.32 ±0.11 cm width, and 0.62 ±0.20 cm height. Surprisingly, no significant differences were detected ($p > 0.05$) between the gland's size and the animal's sex and age, brain size or body weight.

Gross anatomy of the pineal gland

The morphological features of the pineal gland, including shape, color, structure, position, and relations were fully identified using the anatomic sections. The pineal gland in the donkey was an unpaired organ, brown to dark brown in color, and it was found in the midline of the brain. This gland consisted of body and recess. The pineal body appeared elliptical in shape, and it projected dorsally into the third ventricle in a depression between the two thalami and rostral to the rostral colliculi. This body rested on the mesencephalic roof, and it connected to the commissure of the habenulae by two transverse fibers (habenulea) (Figures 1, 2). Moreover, the pineal body extended caudodorsally ventral to the splenium of the corpus callosum. On the sagittal MR image, the pineal body was separated from the splenium of the corpus callosum by the dentate gyrus (Figure 1), while on the transverse MR image, this body was surrounded on both sides by the hippocampus (Figure 2). Furthermore, the pineal recess is an extension of the third ventricle into the pineal gland (Figures 1, 2).

Magnetic resonance imaging of the pineal gland

The gained anatomic data were used as a guide for a precise identification of the MR images. The pineal body could be depicted with intermediate signal intensity on T1-weighted and T2-weighted MR images, and low signal intensity on Flair MR images. The habenulae appeared with intermediate signal intensity on T1-weighted and Flair, and high signal intensity on T2-weighted MR images (Figures 1, 2). Moreover, the pineal recess was filled with cerebrospinal fluid, which appeared with high signal intensity on T2-weighted and Flair, and low signal intensity on T1-weighted MR images (Figures 1, 2).

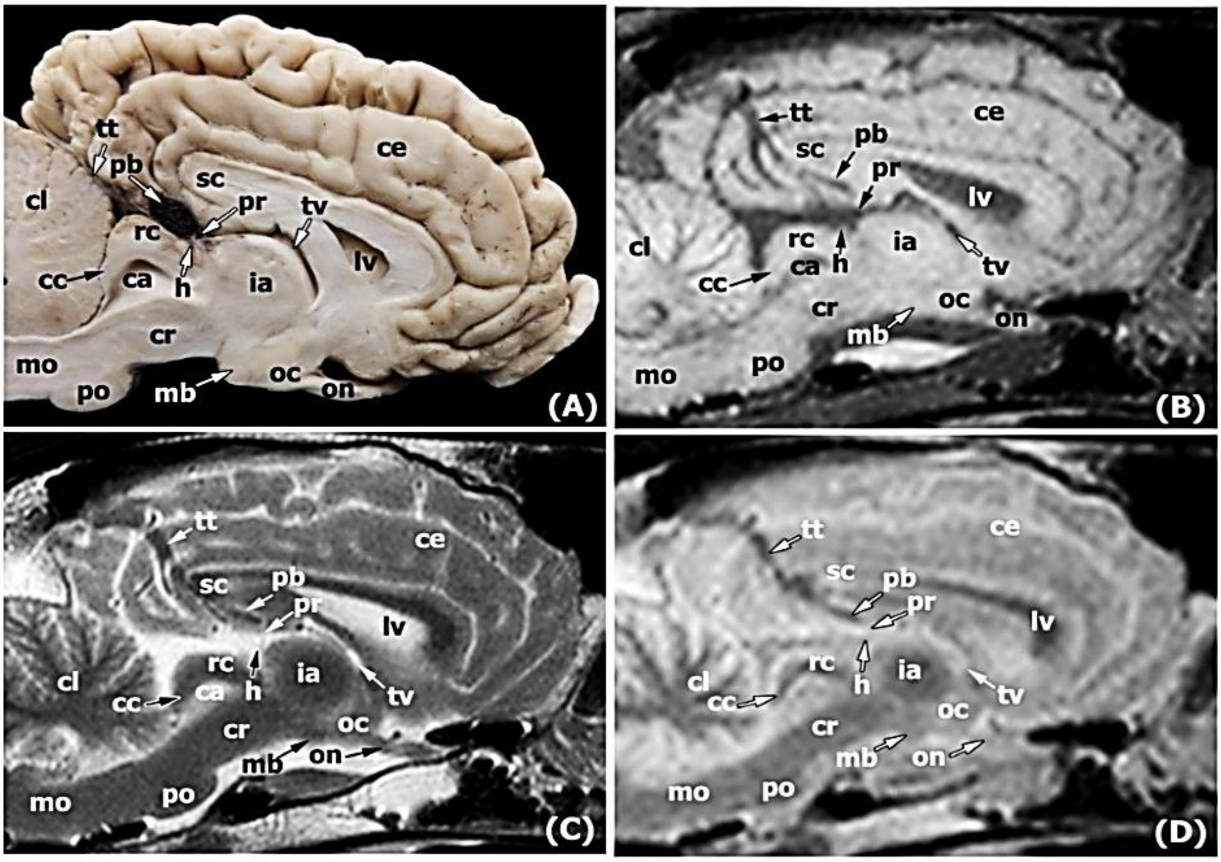

Fig. 1: Sagittal images of the brain in adult donkey at the level of the interthalamic adhesion, sagittal anatomic section (A), T1-weighted MRI image (B), T2-weighted MRI image (C), and Flair MRI image (D). ca- cerebral aqueduct, cc- caudal calliculus, ce- cerebrum, cl- cerebellum, cr- cerebral crus, h- habenula, ia- interthalamic adhesion, lv- lateral ventricle, mb- mamillary body, mo- medulla oblongata, oc- optic chiasma, on- optic nerve, pb- pineal body, pr- pineal recess, po- pons, rc- rostral calliculus, sc- splenium of corpus callosum, tt- tela chordae of third ventricle, tv- third ventricle.

Table 1: Measurements of the brain and pineal gland in 20 adult donkeys (10 males and 10 females).

	Animals' age (years)	Animals' weight (Kg)	Brain length (cm)	Brain width (cm)	Brain Height (cm)	Pineal Length (cm)	Pineal Width (cm)	Pineal Height (cm)
Mean	12.7	176.60	13.89	8.99	6.16	1.23	0.32	0.62
Standard deviation	3.08	17.03	0.21	035	0.21	0.13	0.11	0.20
Standard error	068	3.81	0.04	0.07	0.04	0.03	0.02	0.04

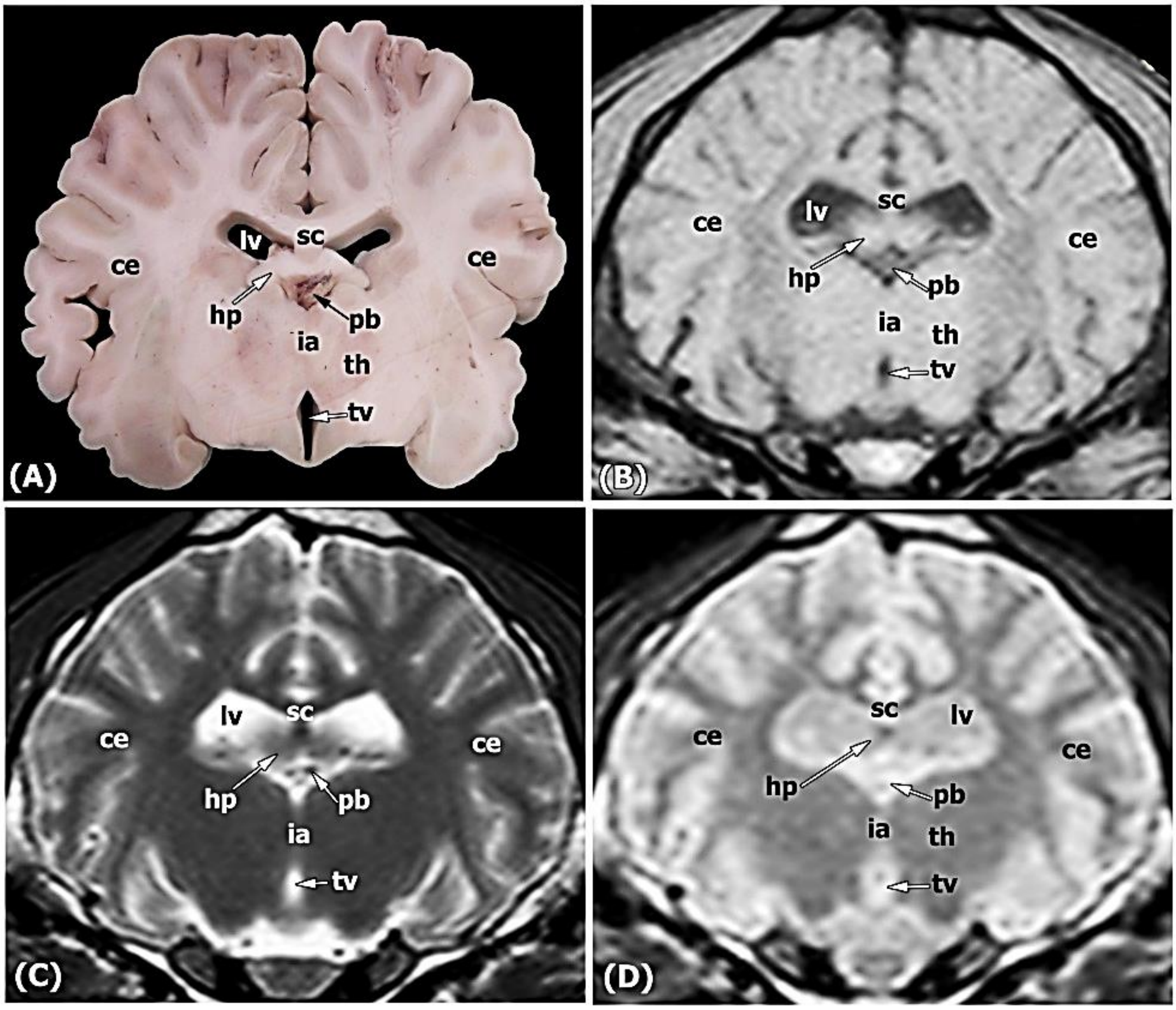

Fig. 2: Transverse images of the brain in an adult donkey at the level of the interthalamic adhesion, transverse anatomic section (A), T1-weighted MRI image (B), T2-weighted MRI image (C), and Flair MRI image (D). ce- cerebrum, hp- hippocampus, ia- interthalamic adhesion, lv- lateral ventricle, pb- pineal body, sc- splenium of corpus callosum, th- thalamus, tv- third ventricle.

DISCUSSION

The current study provided detailed morphometric features and normal magnetic resonance appearance of the pineal gland in donkeys using variable MRI sequences (T1-weighted, T2-weighted, and Flair). The results revealed that the mean size of the pineal gland in donkeys was 1.23 ±0.13 cm length, 0.32 ±0.11 cm width, and 0.62 ±0.20 cm height. Noteworthy that the data about the pineal gland in equines was scarce, anyways the previous studies have reported significant variability in the size of the pineal gland across various animal species: 12.56 mm in length in donkey (Ozgel *et al.,* 2008), 8.83 ±1.07 mm length, 7.91 ±0.83 mm width in buffalo (Carvalho *et al.,* 2009), 12 mm in cattle, and 3-5 mm in sheep (Dursun, 2002). This variability in size might be attributed to the regulatory action of the endocrine system in each species to the circadian cycle and environmental changes. In addition, no significant difference was reported (P>0.05) between the size of the gland and the animal's sex and age, brain size or body weight. These findings are supported by the hypothesis that the size and activity of the mammalian pineal gland were, in fact, affected by geographic position, climate, and light stimulus (Tan *et al.,* 2018).

Morphologically, the current study revealed that the pineal gland consisted of two parts, the body and recess. However, the pineal gland appeared in different forms among species; it consisted of one part, the pineal body, in the donkey (Ebada, 2012). While this gland consisted of three parts with variable descriptions: body, peduncle, and recess in domestic animals (Schaller, 2007), and two lobes (right and left) and a stem in buffalo (Carvalho *et al.,* 2009). Furthermore, an accessory pineal organ is observed in buffalo (Prassad and Sinha, 1984). In addition, the pineal gland under investigation appeared elliptical in shape. However, it appeared fusiform in donkey (Ozgel *et al.,* 2008; Ebada, 2012), lanceolated-shape (Schmidt *et al.,* 2019) or chisel (Dursun, 2002) in horse, rounded in buffalo (Carvalho *et al.,* 2009), wheat green in cattle and flattened pea in sheep (Dursun, 2002; Yildiz *et al.,* 2004), and lancet in dog (Dursun, 2002).

The pineal gland in our study was found between the two thalami in the third ventricle, rostral to the rostral colliculi, and it extended caudodorsally, ventral to the splenium of the corpus callousum. A similar position of the penile gland was reported in other mammals (Dursun, 2002; Yildiz *et al.,* 2004; Ozgel *et al.,* 2008; Ebada, 2012). This close vicinity of the pineal gland to the third ventricle is classified into Type A (Vollrath, 1979). However, in rodents, the pineal gland has deep and superficial parts; the deep part is found in the epithalamic region, while the superficial part is found between the cerebral cortex and cerebellum, and was classified as Type AB (Falcon *et al.,* 2009).

Pinealitis is a common affection of the pineal gland in horses that is associated with recurrent uveitis (Kalsow *et al.,* 1999). Diagnosis of the affected pineal glands requires using highly definitive diagnostic tools. Ultrasonography and traditional radiography have limited applications in the diagnosis of neurological disorders (Mandato *et al.,* 2012; Perrotta *et al.,* 2016). Magnetic resonance imaging is considered an essential tool for instrumental diagnosis and interventional radiology, particularly in the neuroradiological fields (Perrotta *et al.,* 2016; Jarre *et al.,* 2017). In addition, MRI is effectively used as a diagnostic tool for evaluation and prognosis of neurological disorders (Barile *et al.,* 2018; Arnold and Matthews, 2002). However, several previous studies discussed the normal and diseased features of the pineal gland in humans using MRI (Caldas *et al.,* 1985; Gheban *et al.,* 2019). Although scarce studies were available describing the neuroradiological appearance of the pineal gland of the domestic animals, especially in donkeys, the current study permitted a high-definitive visualization of the pineal gland in donkeys in three sequences of MRI, T1-weighted, T2-weighted, and Flair. The obtained MR images in our study were selected with their matched anatomic sections in two planes, sagittal and transverse, at the level of the interthalamic adhesion, providing a comprehensive depiction of the pineal gland and allowing clinicians to properly identify the lesion and interpret the pineal gland from multiple angles. The gross sections in the current study provided a systemic orientation of the normal anatomical features of the pineal gland and helped in the identification and evaluation of the MR images. Moreover, using various MRI sequences allowed a high degree of definition and delineation of the normal anatomic structures, helping accurate diagnosis and prognosis of several pathological conditions (El Nahas *et al.*, 2024). In our study, we used three sequences of MRI, T1-weighted, T2-weighted, and Flair, which enhanced a definitive delineation of the normal pineal gland in donkeys, where it could be depicted with intermediate signal intensity on T1-weighted and T2-weighted MR images and low signal intensity on Flair MR images. However, the normal pineal gland in humans showed isointense on both T1-weighted and T2-weighted MR images (Caldas *et al.,* 1985). Identification of the normal signal intensity of the pineal gland would help in a precise interpretation and evaluation of the tissue changes in the diseased gland. Consequently, the given data could help as a standard reference for future clinical MRI of the pineal gland in donkeys.

CONCLUSION

The present investigation provided a brief morphometric description and a high-definitive MRI visualization of the pineal gland in donkeys. The mean pineal gland size was 1.23 ±0.13 cm length, 0.32 ±0.11 cm width, and 0.62 ±0.20 cm height, proving that no significant differences were detected (P>0.05) between the gland's size and animal's sex and age, brain size or body weight. According to its position in the third ventricle, rostral to the rostral calliculi, the pineal gland in the donkey could be classified into Type A and subclosal in position, as it extended caudoventrally ventral to the corpus callosum. Moreover, the pineal gland could be visualized with variable intensities on different MRI sequences (T1-weighted, T2-weighted, and Flair). These anatomical features of the pineal gland could be used as a standard anatomic reference for further interpretation of the diseased pineal gland in donkeys using MRI.

ACKNOWLEDGEMENTS

The authors would like to thank the radiology team, El-Eman Scan Radiology Center, Beni-Suef Governorate, for performing MRI scanning.

CONFLICT OF INTEREST

The authors have no conflict of interest.

REFERENCES

Arnold, D.L. and Matthews, P.M. (2002): MRI in the diagnosis and management of multiple sclerosis. Neurology. 23(8): 23-31. https://doi.org/10.1212/wnl.58.8_suppl_4.s23

Barile, A.; Reginelli, A.; De Filippo, M.; Brunese, L. and Masciocchi, G. (2018): Diagnostic imaging and intervention of the musculoskeletal system: State of the art. Acta Biomed., 89(1): 5-6. https://doi.org/10.23750/abm.v89i1-S.7006

Bolat, D.; Kurum, A.; Bahar, S. and Karahan, S. (2018): Histomorphometric examination of the pineal gland in foals and adult horses. Ankara Univ. Vet. Fak. Derg., 65(2): 205-212. https://doi.org/10.1501/Vetfak_0000002848

Caldas, J.G.; Doyon, D.; Lederman, H. and Carlier, R. (1985): Magnetic resonance study of the pineal region: normal pineal gland, simple cyst. Arq. Neuropsiquiatr., 56(2): 237-244.

Calvo, J.; Bop, J. and Garcia-Mauriiio, E. (1988): Ultrastructure of the pineal gland in the adult dog. Journal of Pineal Research. 5(5): 479-487. https://doi.org/10.1111/j.1600-079x.1988.tb00790.x.

Carvalho, A.F.; Ambrosio, C.E.; Miglino, M.A.; Mancanares, C.A. and Blazquez, F.J. (2009): Macro-Microscopical aspects of the buffalo (Bubalisbubalis Linnaeus, 1758) pineal gland. Biotemas. 22(2): 127-135. https://doi.org/10.5007/2175-7925.2009v22n2p127

Dahran, N. and Ghonimi, W. (2023): Cytodifferentiation of pinealocytes (I and II) and astrocyte types of mature male sheep epiphysis cerebri with special emphasis on the presence of neuronal and pigmented-like cells. Open Veterinary Journal, Vol., 13(2): 206-217. https://doi.org/10.5455/OVJ.2023.v13.i2.9

Dursun, N. (2002): Veterinary anatomy III, p. 41-42. Ankara: Baski, Medisan, Yayinevi.

Ebada, S. (2012): Morphological and Immunohistochemical Studies on the Pineal Gland of the Donkey (*Equus asinus*). J. Vet. Anat., 5(1): 47-74. https://doi.org/10.21608/JVA.2012.44883

El Nahas, A.; Almohamad, Z. and Hagag, U. (2024): Ultrasonography, computed tomography and magnetic resonance imaging of the dromedary camel distal limbs. BMC Vet. Res., 20(12): 1-9. https://doi.org/10.1186/ s12917-023-03855-2.

Falcon, J.; Besseau, L. and Fuentes, M. (2009): Structural and functional evolution of the pineal melatonin system in vertebrates. Ann. NY Acad. Sci., 1163(1): 101-111. https://doi.org/10.1111/j.1749-6632.2009.04435.x

Frandson, R.D.; Wilke, W.L. and Fails, A.D. (2009): Anatomy and physiology of farm animals. 7th ed. p. 449-456. Iowa, USA: Willy-Blackwell.

Gheban, B.A.; Rosca, I.A. and Crisan, M. (2019): The morphological and functional characteristics of the pineal gland. Medicine and Pharmacy Reports. 92(3): 226-234. https://doi.org/10.15386/mpr-1235

Hussain, M.; Kausar, R.; Qureshi, A.S. and Jamil, H. (2023): Age-Related gross and histomorphometrical dynamics of pineal gland (Epiphysis cereberi) associated with melatonin profile in beetal goat (Capra aegagrus hircus) of Pakistan. Pak. Vet. J., 43(3): 531-536. http://dx.doi.org/10.29261/pakvetj/2023.051

Jarre, A.; Salvador, R.L.; Fornas, G.M. and Filardi, A.M. (2017): Value of brain MRI when sonography raises suspicion of agenesis of the corpus callosum in fetuses. Radiologia. 59(3): 226-31. http://dx.doi.org/10.1016/j.rx.2017.01.002

Kalsow, C.M.; Dubielzig, R.R. and Dwyer, A.E. (1999): Immunopathology of pineal glands from horses with uvetis. IOVS. 40 (7): 1611-1615.

Klein, D.C. (2015): The pineal gland and melatonin. In Sperling, M.A., Endocrinology: adult and pediatric. p. 1072. Philadelphia: Elsevier.

Koshy, S.G. and Vettivel, S. (2001): Melanin pigments in human pineal. J. Anat. Soc., 50(2): 122-126.

Mandato, Y.; Reginelli, A.; Galasso R.; Iacobellis, F.; Berritto, D. and Cappabianco, S. (2012): Errors in the Radiological Evaluation of the Alimentar Tract: Part I. Semin Ultrasound CT MR, 33(4): 300-307. http://dx.doi.org/10.1053/j.sult.2012.01.011.

Ozgel, O.; Dursun, N. and Oto, C. (2008): The morphology and arterial vascularization of the pineal gland in donkeys. Journal of Animal and Veterinary Advances, 7(11): 1511-1514.

Perrotta, F.M.; Astorri, D. and Zappia, M. (2016): An ultrasonographic study of enthesis in early psoriatic arthritis patients naïve to traditional and biologic DMARDs treatment. Rheumatol. Int., 36(11): 1579-83. http://dx.doi.org/10.1007/s00296-016-3562-

Peterfy, C.G.; Linares, R. and Steinbach, L.S. (1994): Recent advances in magnetic resonance imaging of the musculoskeletal system. Radiol. Clin. North Am., 32(2): 291-311.

Phillips, T.S.; Tsin, A.T.: Reiter, R.J. and Malsbury, D.W. (1989): Retinoids in the bovine pineal gland. Brain Research Bulletin. 22(2): 259-261. https://doi.org/10.1016/0361-9230(89)90051-8

Phuttharak, W.; Wannasrnmetho, M.; Lueanginghasut, P.; Waraasawapati, S. and Mukherji, S.K. (2023):

Differentiation between germinoma and other pineal region tumors using diffusion-and susceptibility-weighted MRI. European Journal of Radiology, 159(110663): 1-9. https://doi.org/10.1016/j.ejrad.2022.110663

Prassad, J. and Sinha, R.D. (1984): Histological and histochemical studies on the pineal and accessory pineal bodies in buffalo. Indian Journal Animal Science. 54 (1); 45-49.

Schaller, O. (2007): Illustrated veterinary anatomical nomenclatures, 2nd ed. p.443-444. Germany: Stuttgart Gmbh.

Schmidt, M.J.; Knemeyer, C. and Heinsen, H. (2019): Neuroanatomy of the equine brain as revealed by high-field (3Tesla) magnetic-resonance-imaging. PLoS ONE. 14(4): e0213814. https://doi.org/10.1371/journal.pone.0213814

Simonneaux, V. and Ribelayga, C. (2003): Generation of the melatonin endocrine message in mammals: a review of the complex regulation of melatonin synthesis by norepinephrine, peptides, and other pineal transmitters. Pharmacol Rev., 55(2): 325–395. https://doi.org/10.1124/pr.55.2.2

Tan, D.X.; Xu, B.; Zhou, X. and Reiter, R.J. (2018): Pineal calcification, melatonin production, aging, associated health consequences and rejuvenation of the pineal gland. Molecules. 31;23(2): 301.https://doi.org/10.3390/molecules23020301

Werpy, N.M. (2004): Magnetic resonance imaging for diagnosis of soft tissue and osseous injuries in the horse. Clin Tech Equine Pract., 3(2): 389-98. https://doi.org/10.1016/j.cveq.2018.04.009

Vollrath, L. (1979): Comparative Morphology of the Vertebrate Pineal Complex. Progress in Brain Research. 52, 25-38. https://doi.org/10.1016/S0079-6123(08)62909-X

Yildiz, D.; Gultiken, M.E. and Bolat, D. (2004): Arterial supply of the pineal gland in Akkaraman sheep. Acta. Vet. Hung., 52(1): 1-6. https://doi.org/10.1556/AVet.52.2004.1.1.

تصوير الغدة الصنوبرية بالرنين المغناطيسي في الحمار (*Equus asinus*)

محمد كمال مرعى عبد المقصود ، هيوا محمد على ، عزة على حسن ابراهيم ، هبة الله حمدى محمود

Email: mkamalvet@gmail.com Assiut University web-site: www.aun.edu.eg

الغدة الصنوبرية في الثدييات، هي غدة صغيرة عصبية صماء، تنظم الإيقاع اليومي والنشاط التناسلي في الحيوانات التي تتكاثر موسميًا. تهدف الدراسة الحالية إلى توضيح الخصائص القياسية الشكلية للغدة الصنوبرية وتقييم خصائصها الطبيعية باستخدام صور الرنين المغناطيسي (MRI) بمتواليات مختلفة في الحمير. تم استخدام رؤوس جثث لاثنين وعشرين حمارًا بالغًا دون أي علامات عصبية غير طبيعية. تم فحص رأسين باستخدام جهاز رنين مغناطيسي بقوة ١,٥ تسلا بثلاث متواليات (T1-weighted, T2-weighted, Flair)، ثم تم حفظهما في محلول فورمالين بنسبة ١٠٪ لمدة عشرة أيام. بعد ذلك تم تقطيع أدمغة هذه الرؤوس المحفوظة إلى شرائح عرضية وطولية. تم استخراج أدمغة العشرين رأسًا الأخرى بعناية، وتم قياس وزنها وطولها وعرضها وارتفاعها. كما تم قياس عرض وطول وارتفاع الغدة الصنوبرية في هذه العينات وربطها بجنس الحيوان وعمره وحجم الدماغ ووزن الجسم باستخدام اختبارات إحصائية مختلفة. كان متوسط حجم الغدة الصنوبرية ١,٢٣ ± ٠,١٣ سم طولًا، ٠,٣٢ ± ٠,١١ سم عرضًا، و٠,٦٢ ± ٠,٢٠ سم ارتفاعًا. لم يتم اكتشاف أي فرق كبير (P>0.05) بين حجم الغدة وجنس الحيوان أو عمره أو حجم الدماغ أو وزن الجسم .ساعدت المقاطع التشريحية للدماغ في الوصف الشكلي للغدة الصنوبرية، بما في ذلك لونها وشكلها وموقعها وعلاقاتها. علاوة على ذلك، سمح استخدام متواليات مختلفة من الرنين المغناطيسي (T1, T2, Flair) بتقييم شامل للغدة الصنوبرية بكثافات مختلفة. يمكن استخدام هذه الخصائص التشريحية للغدة الصنوبرية كمرجع تشريحي قياسي لتفسير أمراض الغدة الصنوبرية في الحمير.